On absolute phase determinant ion techniques in SAR interferometry

Søren N. Madsen

Jet Propulsion Laboratory, California Institute of Technology
4800 Oak Grove Dr., Pasadena, CA 91109

ABSTRACT

Cross-track interferometric SAR can provide 3-dimensional radar images. The technique relies on determining the target elevation from the difference in slant range observed by two antennas having, across-track separation. The range differences estimated very precisely using the phase difference observed in an interferogram obtained from the two complex images. A key problem is that the range difference can only be determined to within a multiple of the wavelength, as the phase difference is measured modulo 2π. This paper discusses two different methods to determine the unknown multiple of 2π: l) the split-spectrum algorithm, and 2) the residual delay estimation algorithm. The Split-spectrum algorithm utilizes the carrier frequency dependence of the interferometric phase, as subdividing the available range bandwidth into two bands provides two slightly different interferograms. The phase difference of the interferograms corresponds to an interferogram obtained with a system having a carrier frequency which is the difference between the two band centers. The residual delay estimation method is based on the full bandwidth, one-look images used to formthei nterferogramand involves precision interpolation and coregistration steps. Principles are presented, along with possible implementations of the algorithms. Principal error sources, as well as advantages and disadvantages from a processor design and implementation point of view are also discussed.

Keywords: SAR interferometry, synthetic aperture radar (SAR), absolute phase, split-spectrum algorithm, residual delay estimation algorithm

1 INTRODUCTION

Topographic maps can be generated using interferometric SAR as demonstrated by Graham', and Zebker and Goldstein*, Organizations like NASA's Jet Propulsion Laboratory (JPL) and the Canada Centre for Remote Sensing (CCRS) have been flying single-pass airborne interferometric SAR for several years [3,4] and several other organizations are presently developing interferometric SAR systems. Also, satellite SAR systems have been used for several years for generating topographic maps using a single sensor in the repeat-pass mode [2,5]. Recently, other uses of interferometric SAR techniques, including measurement of dynamic phenomena have been investigated [6,7,8]. Airborne interferometric topographic SAR has the potential to provide high resolution; horizontal and vertical accuracies on the order of a meter are feasible today [9]. Radar techniques for the generation of precision topographic maps have several advantages compared to traditional stereo photography including: all weather, day and night capability, the possibility of fast automated processing systems for generating high resolution maps; and the potential to provide absolute location without the use of known ground reference points. The production of high quality topographic maps from interferometric SAR data depends on the solution of a number of technical issues, such as: 1) availability of accurate platform positions and interferometric baseline estimates (length and attitude); 2) Implementation of motion compensation in the processing; 3) preservation of relative signal phases in the processor; 4) a 3-dimensional location algorithm; and 5) implementation of an algorithm to derive the absolute phase. Only the last point will be discussed here, points 1 through 4 has been discussed previously [10].

Consider a simplified situation with a SAR flying along a straight line with the antenna pointed orthogonal to the velocity vector (zero Doppler geometry). Azimuth processing will in this case separate the observed targets into planes orthogonal to the flight direction. The two interferometer antennas are displaced by $\vec{r}_{21}$ which must have a significant component orthogonal to both the velocity and the line-of-sight vector, The two antenna locations are

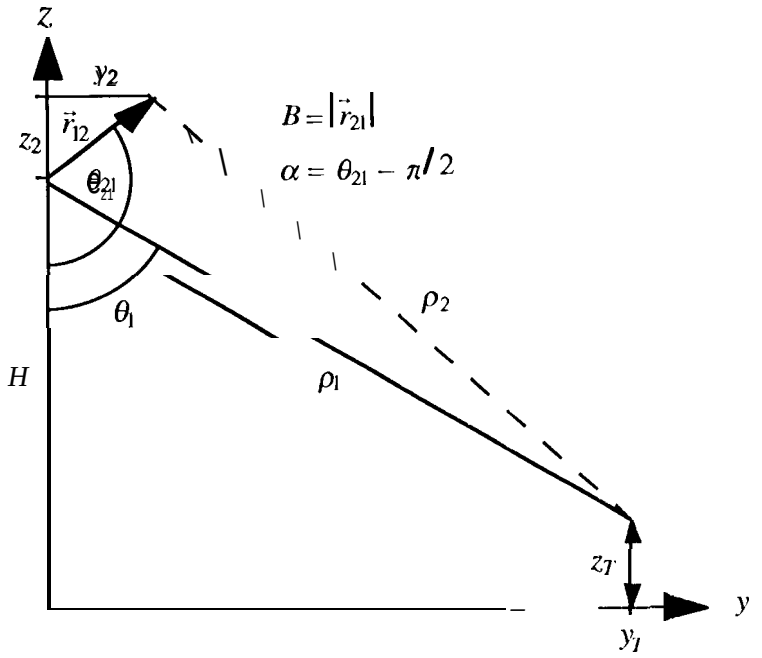

Figure 1. The data acquisition geometry of an cross-track interferometric, topographic mapper (the platform would be flying into, or out of, the paper).

known, as well as the slant ranges from antennas 1 and 2 to the target, and the target location can be determined by simple triangulation (see Figure 1), However, with a baseline typically on the order of a thousandth of the slant range, it is easily seen that to determine the across line-of-sight position well, the slant range difference must be known very accurately. A key element in the interferometric method is that the slant range difference is directly proportional to the absolute phase difference of the two received signals. The phase difference at each point on the surface is measured by multiplying the complex image generated from antenna 1 data by tile complex conjugate of the data generated from antenna 2 data. This, unfortunately, only provides the phase modulo 2π. Goldstein *et al.*[4] developed a technique to unwrap the absolute interferometric phase except for a multiple of 2n which would be the same over the entire area unwrapped. In combination with one reference point with known position—which must be recognizable in the radar image-this phase offset can be calculated and the elevations of all image points can be found. The following sections will discuss methods to determine the absolute phase without the use of ground reference points.

2 THE ABSOLUTE PHASE

Using the geometry of Figure 1, the relationship between the geometrical parameters of interest (y_T, z_T) and the observable $(P_1, \rho_2, \phi_{wrap})$, $\phi_{wrap} = 1 - z + \pi]$, can be derived. The following relations will suffice for the discussion here,

$$\begin{aligned} \Delta\rho = \rho_2 - \rho_1 &\approx -|\vec{r}_{21}|\cos(\theta_{21} - e,) \\ z_T &= H - \rho_1 \cos\theta_1 \\ y_T &= \rho_1 \sin\theta_1 \end{aligned} \tag{1}$$

and the phase of the interferogram (the interferogram defined as channel 1 times the complex conjugate of channel 2) is,

$$\phi = \phi_1 - \phi_2 = -2\pi f_0 (t_{d1} - t_{d2}) = \frac{2\pi p}{\lambda}(\rho_2 - \rho_1) \qquad \phi_{\text{wrap}} = \text{mod}(\phi, 2\pi) \tag{2}$$

where f_0 is the carrier frequency, λ is the wavelength, and p is a multiplier; p = 2 for two-way propagation differences (both transmitter and receiver is different for the two channels), $p = 1$ if the two channels share a common receiver. The phase directly available in the complex interferogram is the absolute phase modulo 2π. *The expression "absolute phase" is used here to denote a phase which is directly proportional to the slant range difference.*

To understand the algorithms proposed for determining the absolute phase, the expressions for the signals forming the interferogram will be derived in the following. The transmitted signal, *p(t),* is given by,

$$pi(t) = h_i(t)\exp(j2\pi f_0 t) \tag{3}$$

$h_i(t)$ is the modulating function for the signal transmitted by channel i (= 1 or 2). Note that to the extent the receiver modifies the transfer function, this will be included in *hi(t)* here. The received signal is

$$r_i(t) = p_i(t - t_{di}) = h_i(t - t_{di})\exp(j2\pi f_0 (t - t_{di})) \tag{4}$$

where the time delay is given by

$$t_{di} = \frac{2}{c}\sqrt{(y_i - y_T)^2 + (H + z_i - z_T)^2} \tag{5}$$

After down-conversion the baseband signal is

$$b_i(t) = h_i(t - t_{di})\exp(-j2\pi f_0 t_{di}) \tag{6}$$

As part of the signal processing it is necessary to motion compensate the data (that is, correct for the fact that the flight path is not a straight line or a great circle arc.), and to register the two data channels such that the images forming the interferogram overlay as accurately as possible without knowing the actual target elevation; for more detail see Madsen *et al.* [10]. For both motion compensation and coregistration, the purpose of the signal processing is to transform the received data to a signal at a different time delay. This data transformation can be implemented in a number of ways, however, it is found that applying a shift of the baseband signal and phase correction which corresponds *exactly* to the shift (equivalent to shifting the signal at the carrier frequency) makes the implementation of the absolute phase determination algorithms simpler.

In the following the motion compensation for both interferometric channels uses a common reference line, denoted track O. in this case the shift and phase correction required to properly focus the image in azimuth will at the same time nominally overlay the two images correctly, "Nominally" her e implies that if all targets are at a specific reference target height assumed in the processing, then there are no misregistration errors. Motion compensation and channel registration can thus be achieved by calculating the slant range from a "nominal" target at the reference height to track O and the actual radar path respective y, and shifting and phase correcting the received data accordingly. Note that the motion compensation target reference is not in general coincident with the actual target coordinates. The time delay from the nominal target to the actual radar track is

$$t_{di,REF} = \frac{2}{c}\sqrt{(y_i - y_{REF})^2 + (H + z_i - z_{REF})^2} \tag{7}$$

and the time delay from the nominal target to the reference track, track O, is

$$t_{d0,REF} = \frac{2}{c}\sqrt{(y_{REF})^2 + (H - z_{REF})^2} \tag{8}$$

The signal will after the slant range shift and the phase correction be given by

$$\begin{aligned} g_i(t) &= h_i(t - t_{di,REF} - t_{d0,REF} - t_{di}) \exp(j2\pi f_0 (t_{di,REF} - t_{d0,REF} - [,/,)) \\ &= b_i(t + t_{di,REF} - t_{d0,REF}) \exp(j2\pi f_0 (t_{di,RI F} - t_{d0,REF})) \end{aligned} \quad \textbf{(9)}$$

resulting in the following expression for the interferogram formed:

$$\begin{aligned} c(t) = g_1(t)\bar{g}_2(t) = h_1(t - t_{d1} + t_{d1,REF} - t_{d0,REF}) \bar{h}_2(t - t_{d2} + t_{d2,REF} - t_{d0,REF}) \\ \exp(j2\pi f_0(t_{d1,REF} - t_{d2,REF})) \exp(j2\pi f_0(t_{d2} - t_{d1})) \end{aligned} \quad \textbf{(lo)}$$

In general h_i does not have to be real valued. In fact, for the split-spectrum algorithm it is useful to understand the effect of a modulation function on a carrier frequency. Let

$$\text{hi(f)} = h_{0i}(t) \exp(j2\pi f_{\text{offset}} t) \quad (11)$$

where h_0 is real valued and the phase due to the modulation function carrier, f_{offset}, now written out explicitly. The baseband signal is then, after slant range shift and phase correction,

$$\begin{aligned} g_i(t) = h_{0i}(t - t_{di} - t_{di,REF} - t_{d0,REF}) \exp(j2\pi f_{\text{offset}} (t + t_{di,REF} - t_{d0,REF})) \\ \exp(j2\pi f_0 (t_{di,REF} - t_{d0,REF})) \exp(-j2\pi (f_0 + f_{\text{offset}}) t_{di}) \end{aligned} \quad \textbf{(12)}$$

and the interferogram is given by

$$\begin{aligned} c(t) = g_1(t)\bar{g}_2(t) = h_{01}(t - t_{d1} + t_{d1,REF} - t_{d0,REF}) h_{02}(t - t_{d2} + t_{d2,REF} - t_{d0,REF}) \\ \exp(-j2\pi (f_0 + f_{\text{offset}})(t_{d1} - t_{d2} - (t_{d1,REF} - t_{d2,REF}))) \end{aligned} \quad (13)$$

This expression shows that the interferogram phase is proportional to the actual carrier frequency of the signals used to form the interferogram and the difference between the actual time delay differences and those assumed in the motion compensation/coregistration correction. This result might seem trivial and even self evident from equation (1 O). The interesting observation is, however, that the actual down conversion frequency is not a factor at all, and this is a consequence of the motion compensation approach taken (with the exact correspondence between the shift and the phase shift). This leads to the following expression for the interferogram

$$\begin{aligned} c(t, f) = g_1(t)\bar{g}_2(t) = h_{01}(f - t_{d1} + t_{d1,REF} + t_{d0,REF}) \bar{h}_{02}(t - t_{d2} + t_{d2,REF} - t_{d0,REF}) \\ \exp(-j2\pi f(t_{d1} - t_{d2} - (t_{d1,REF} - t_{d2,REF}))) \end{aligned} \quad (14)$$

where, hoi is the low-pass version of the modulation function and f is the effective carrier frequency. For now, it will be assumed that the sensor is error free (error sources are discussed in section 5), and it is assumed that the low-pass transfer functions are identical, real and symmetrical, which means that the phase of $h_{01}h_{02}$ is always zero, and that the cross-correlation function of $h_{o1}(t)$ and $h_{02}(t)$ *is* symmetrical with its maximum at $t = O$.

3 SPLIT-SPECTRUM ALGORITHM FOR ABSOLUTE PHASE I}KTERM1NATION

This section is devoted to a discussion of the split-spectrum algorithm [12] which was probably the first algorithm used for estimating the absolute interferometric phase from the radar data without the usc of ground information.

3.1 Theory

The key to the split spectrum algorithm is the observation that the interferogram phase is proportional to the transmitted carrier frequency, as seen from equation (14). Using the motion compensation and coregistration approach outlined earlier (equation (9)), the actual baseband frequency is irrelevant; only the carrier frequency is important. By filtering

the range spectrum as part of the digital range compression of the received signal, the full range spectrum can be subdivided into two (or more) channels corresponding to different carrier frequencies. For instance, a rectangular spectrum centered at f_0 with a total bandwidth of $2B$ can be separated into two channels, with carrier frequencies $f_+ = f_0 + B/2$ and $f_- = f_0 - B/2$ respectively, both with a bandwidth B. A differential interferogram generated from two interferograms, at carrier frequencies f_+ and f_-, is given by

$$\begin{aligned} d(t, f_+, f_-) = c(t, f_+)\bar{c}(t, f_-) = {} & h_{01}^{f_+}(t - t_{d1} + t_{d1,REF} - t_{d0,REF})\, \bar{h}_{02}^{f_+}(t - t_{d2} + t_{d2,REF} - t_{d0,REF}) \\ & \bar{h}_{01}^{f_-}(t - t_{d1} + t_{d1,REF} - t_{d0,REF})\, h_{02}^{f_-}(t - t_{d2} + t_{d2,REF} - t_{d0,REF}) \\ & \exp(-j2\pi(f_+ - f_-)(t_{d1} - t_{d2} - (t_{d1,REF} - t_{d2,REF}))) \end{aligned} \tag{15}$$

As the low-pass modulation function does not contribute to the phase, it is seen that the phase of the differential interferogram is equivalent to that of an interferogram with a carrier which is the difference of the carrier frequencies of the two interferograms combined. Thus the phase of an interferogram corresponding to a carrier frequency f_- is

$$\phi_0(t) = -2\pi f_0(t_{d1} - t_{d2} - (t_{d1,REF} - t_{d2,REF})) \tag{16}$$

and the phase of a differential interferogram with carrier frequencies f_+ and f_- is

$$\phi_{+/-}(t) = -j2\pi(f_+ - f_-)(t_{d1} - t_{d2} - (t_{d1,REF} - t_{d2,REF})) \tag{17}$$

It is assumed in the following that $f_+ - f_-$ is chosen such that the differential phase is always in the range $[-\pi, +\pi[$ thus making the differential phase unambiguous, A different way of stating that requirement is that the wavelength corresponding to the frequency difference $f_+ - f_-$ should be larger than the physical baseline times p (the multiplier accounting for one- or two-way patch differences). Equations (16) and (17) can be combined to

$$\frac{\phi_{+/-}(t)}{f_+ - f_-} = \frac{\phi_0(t)}{f_0} \Leftrightarrow \phi_{+/-}(t) = \phi_0(t)\frac{f_0}{f_+ - f_-} \tag{18}$$

which shows that the absolute phase, ϕ_0, can, at least in principle, be derived from the unambiguous differential interferogram phase.

3.2 **Implementation**

Unfortunately, the noise on the differential interferogram is larger than that of the "standard" interferogram. The thermal noise on either interferogram used to form the differential will be larger by typically $\sqrt{2}$ due to the smaller number of looks, and combining 2 interferograms with independent noise increases the noise by another factor of $\sqrt{2}$, such that the rms phase error on the differential interferogram is typically a factor of 2 larger than on the "standard" interferogram. The noise on the differential interferogram is further amplified by the factor $f_0/(f_+ - f_-)$ which is usually very large, However, by averaging over an entire image, it is still possible to achieve the required accuracy. First note that in combination with the unwrapped phase

$$\phi_{unw}(t) = \phi_0(t) - n2\pi \tag{19}$$

equation (18) can be reformulated to give the residual number of 2π's by which the unwrapped phase differs from the absolute phase

$$n = \frac{1}{2\pi}\left(\phi_{+/-}(t)\frac{f_0}{f_+ - f_-} - \phi_{unw}(t)\right) \tag{20}$$

This expression applies for the entire unwrapped image, thus even if the estimate of n on a pixel to pixel basis is very noisy, averaging over the image can usually provide a sufficiently accurate estimate for n, for typical system

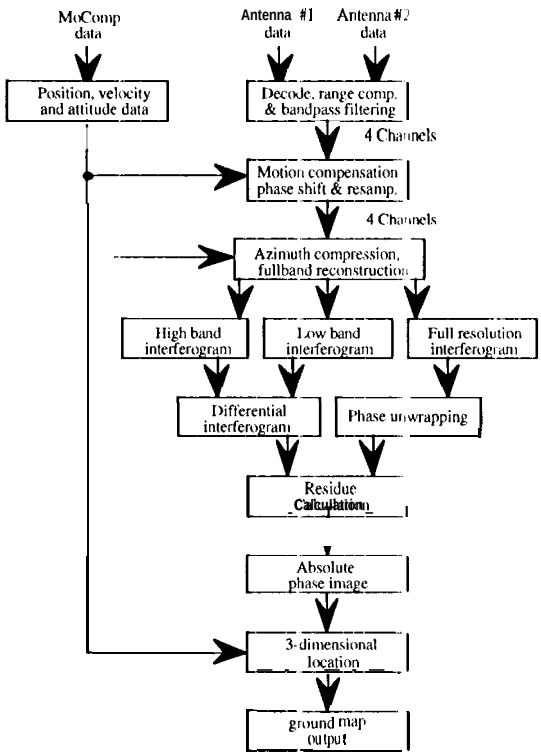

Figure 2. Topographic interferometric SAR processing system lay-out based on the split-spectrum algorithm for absolute phase determination.

parameters, as for instance the JPL TOPSAR system [12]. (Sufficiently accurate means that the estimation noise must be less than 0.5.) An implementation of the split-spectrum algorithm is shown in Figure 2. A draw-back in using the split-spectrum algorithm is that a total of 4 one-look complex images needs to be processed to form the differential interferogram. An alternative approach is to process two full bandwidth images up to the interferogram formation, and then band-pass filter the single look images at this stage. This approach has been found to generate less accurate results. This can be ascribed to the changes in the range spectrum caused by the azimuth processing, but the details are outside the scope of this paper.

4 RESIDUAL DELAY ESTIMATION METHOD

The residual delay estimation method was originally developed to reduce the amount of processing overhead required to estimate the absolute phase. Contrary to the split-spectrum algorithm it only requires two complex single look images.

4.1 Theory

The expression for the absolute phase of the full bandwidth interferogram was provided in equation (1 6). The unwrapped phase is given by equation (16) in combination with equation (19),

$$\begin{aligned}\phi_{unw}(t) &= -2\pi f_0(t_{d1} - t_{d2} - (t_{d1,REF} - t_{d2,REF})) - n2\pi \\ &= -2\pi f_0(t_{d1} - t_{d2} - (t_{d1,REF} - t_{d2,REF}) + \frac{n}{f_0})\end{aligned} \tag{21}$$

where n is unknown but constant over the image. Using $\phi_{unw}(t)$, channel 2 can be resampled and phase shifted,

$$g_2^S(t) = g_2(t - \frac{\phi_{unw}}{-2\pi f_0}) \exp(j\phi_{unw})$$

$$= h_2(t - t_{d2} + t_{d2,REF} - t_{d0,REF} - \frac{\phi_{unw}}{-2\pi f_0}) \exp(j2\pi f_0(-t_{d2} + t_{d2,REF} - t_{d0,REF}) + j\phi_{unw}) \quad (22)$$

$$= h_2(t - t_{d1} + t_{d1,REF} - t_{d0,REF} - \frac{n}{f_0}) \exp(j2\pi f_0 (-t_{d1} + t_{d1,REF} - t_{d0,REF} - \frac{n}{f_0}))$$

It is seen that if $h_2(t) = h_1(t)$ then g;(t)= $g_1(t - n/f_0)$. (a symmetrical version, shifting both channels, is a trivial extension.) Thus for a given patch, after resampling and phase shifting one of the one look complex images, the two images will be identical with the exception of a time delay difference (= two times the range difference divided by the speed of light) which is: 1) constant over the image patch processed; and 2) proportional to n, the number of cycles by which the unwrapped phase, ϕ_{unw} differs from the absolute phase. To determine the correct ambiguity number, n, the range delay must be determined with an accuracy better than A/4. For a 5 cm wavelength and a 3.75 m slant range resolution (equivalent to a 40 MHz bandwidth) that requires an accuracy in determining the correlation peak which is better than 1/300 of the resolution. That is a very challenging but not impossible requirement.

4,2 Implementation

The residual delay estimation algorithm can be implemented with only a few modifications to a straight forward interferometric processor architecture, as shown in Figure 3. Note, that if the residual delay estimated is large compared to the slant range resolution, the interferogram calculated will have significant decorrelation due to misregistration. In this case it is necessary to feed the residual phase estimate back to the motion compensation step and redo the processing from that point.

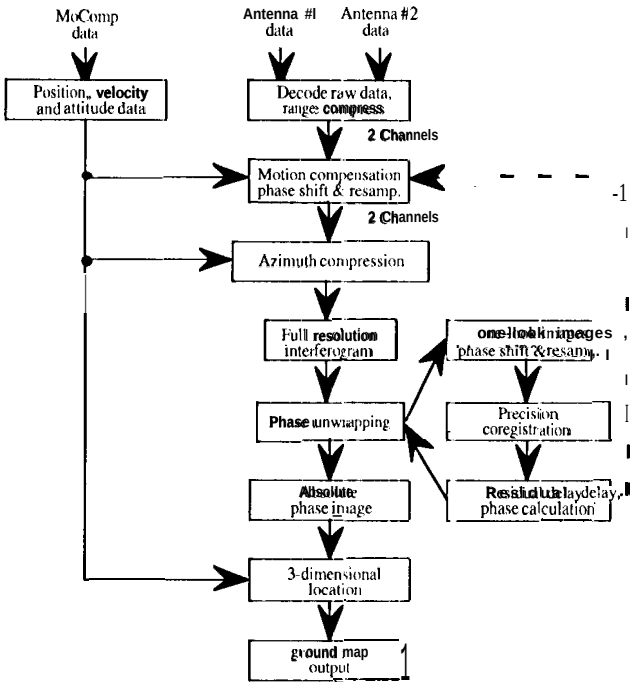

Figure 3 Topographic interferometric SAR processing system lay-out based on the residual delay estimation algorithm for absolute phase determination.

5 ERROR SOURCES

Important error sources will be qualitatively discussed in this section, as a full quantitative discussion of the error sources limiting the accuracy of the absolute phase estimation algorithms proposed is beyond the scope of this paper.

Thermal noise will introduce random errors. By weighting the individual contributions to the ambiguity estimation, the influence of isolated areas with low signal-to-noise-ratio will however be small. If the single-look images used in forming the interferogram are weighted to achieve a uniform signal-to. noise-ratio across the swath this weighting will automatically be achieved by the cross-correlation of the residual delay estimation algorithm. In the case of the split-spectrum algorithm the weighting will have to be explicitly applied.

Interpolation is a key element in the signal processing. If the interpolations in the SAR processor are not implemented carefully, they will modify the transfer functions and introduce systematic errors in the absolute phase estimate. In the case of the split-spectrum estimation even small transfer function changes will have a significant impact on the absolute phase due to the very large multiplier involved ($f_0/(f_+$ ----)). In the case of the residual delay estimator even small changes in the system impulse response function will bias the determination of the cross-correlation peak which is critical when accuracies on the order of a thousandth of a pixel is sought.

System transfer functions are also critical. Ideally the transfer functions $h_{01}(t)$ and $h_{02}(t)$ would be identical, real, and symmetrical. Careful inspection of the expressions derived will, however, show that if h_{01}(t) and $h_{02}(t)$ are identical, and if the coregistration applied in the motion compensation and registration step is fairly accurate then the error induced by lack of symmetry and a non-zero imagenary component, will generally be minimal. In the case of a single-pass cross-track interferometric system that suggests that a system with two identical antennas pointing in the same direction is ideal since the transfer functions imposed by both antennas are identical for any given target. Even in the case where the transfer functions of the two channels are not identical, real, and symmetrical, the artifacts induced can generally be calibrated out if the transfer function is constant across the swath (such invariant errors could for instance be caused by mismatched receivers). However, when the transfer functions of the two channels are different and furthermore varying across the swath, it can be very difficult to estimation the absolute phase accurately,

The analysis outlined in this paper also assumes that the interferogram phase is varying slowly over the extent of the impulse response. Similarly, and quite related, it is assumed that there are few errors in the phase unwrapping process. Both error sources can be significantly reduced by applying, masking techniques which reduce the weight of areas where the interferometric phase is rapidly varying.

6 DISCUSSION

Two algorithms for automatic determination of the absolute phase in SAR interferometry have been proposed. Both algorithms have been implemented and tested in interferometric processors developed at JPL. Presently, the residual delay estimation algorithm is the algorithm of choice, primarily due to the fewer modifications of the standard processing scheme required. For operational processing where computational efficiency is important, the residual delay estimation algorithm is preferred. When processing multiple consecutive patches, which is standard situation in a strip map processor, it is possible to boot-strap from the previous patch and still use the same processing scheme, just skipping the absolute phase estimation. Preliminary indications arc also, that the accuracy of the residual delay estimation algorithm is better. Experimental results are presently being systematically compared and will be presented in the near future.

7 ACKNOWLEDGMENTS

Thanks to Dr. Paul Rosen of JPL for his help in implementing and testing the algorithms and for his comments and corrections to the draft manuscript. The work described in this paper was funded by the Advanced Research Projects Agency (ARPA) and carried out at the Jet Propulsion Laboratory, California 1 nstitute of Technology, under a cent ract with NASA.

8 REFERENCES

[1] Graham, L. C., "Synthetic interferometer radar for topographic mapping," *Proceedings of the IEEE*, Vol. **62, No. 6, pp. 763-768, 1974**

[2] Zebker, H.A. and R.M. Goldstein, "Topographic mapping from interferometric SAR observations," *Journal of Geophysical Research,* Vol. 91, B5, pp. 4993-4999, 1986

[3] Zebker, H.A., S.N. Madsen, J. Martin, K.B. Wheeler, T. Miller, 1.. Yunling, G. Alberti, S. Vetrella, and A. Cucci, "The TOPSAR interferometric radar topographic mapping instrument," *IEEE Trans. Geoscience and Remote Sensing, vol. 30, No. 5,* pp. 933-940, 1992

[4] Gray, A.]., K.E. Mattar, and P.J. Farris-Manning, "Airborne SAR interferometry for terrain elevation," in proceedings of the International Geoscience and Remote Sensing Symposium, lGARSS'92, Vol. 2, pp. 1589–1591, 1992

[5] Zebker, H. A., C. Werner, P.A. Rosen, and S. Hensley, "Accuracy of topographic maps derived from ERS–1 Interferometric radar," *IEEE Trans. Geoscience and Remote Sensing,* Vol. 32, No. 4, pp. 823-836, 1994

[6] Massonnet, D., M. Rossi, C. Carmona, F. Adragna, G. Peltzer, K. Feigi, and T. Rabaute, "The displacement field of the Landers earthquake mapped by radar interferometry," *Nature,* Vol. 364, pp. 138-142, 1993

[7] Goldstein, R. M., H. Engelhardt, B. Kamb, and R.M. Frolich, "Satellite radar interferometry for monitoring ice sheet motion: Application to an Antarctic ice stream," *Science,* Vol. 262, pp. 1525-1530, 1993

[8] Zebker, H. A., P.A. Rosen, R. M, Goldstein, C. Werner, and A. Gabriel, "On the derivation of coseismic displacement fields using differential radar interferometry," *Journal of Geophysical Research–Solid Earth,* Vol. *99, No. 10, pp. 19617-19634, 1994*

[9] Madsen, S. N., J.M. Martin and H.A. Zebker, "Analysis and evaluation of the NASA/JPL TOPSAR across-track interferometric SAR system", *IEEE Trans. Geoscience and Remote Sensing,* Vol. 33, No, 2, 1995

[10] Madsen, S. N., H.A. Zebker and J.M. Martin, "Topographic mapping using, radar interferometry: Processing techniques", *IEEE Trans. Geoscience and Remote Sensing,* Vol. 31, No. 1, pp. 246-256, 1993

[11] Goldstein, R.M., H.A. Zebker, and C.L. Werner, Satellite radar interferometry: Two-dimensional phase unwrapping> *Radio Science,* Vol. 23, No. 4, pp. 713-720, 1988

[12] Madsen, S. N., and H.A. Zebker, "Automated absolute phase retrieval in across-track interferometry," in proceedings of the international Geoscience and Remote Sensing Symposium, IGARSS'92, Vol. 2, pp. 1582–1 584, 1992